Journal of Power Sources 256 (2014) 133–136

Contents lists available at ScienceDirect

Journal of Power Sources

journal homepage: www.elsevier.com/locate/jpowsour

Short communication

Electrochemical characteristics of iron oxide nanowires during lithium-promoted conversion reaction

Inchul Hong [a], Marco Angelucci [b], Roberta Verrelli [a], Maria Grazia Betti [c], Stefania Panero [a], Fausto Croce [d], Carlo Mariani [c], Bruno Scrosati [e], Jusef Hassoun [a,*]

[a] Dipartimento di Chimica, Sapienza Università di Roma, P.le A. Moro 2, I-00185 Roma, Italy
[b] Dipartimento di Fisica, Sapienza Università di Roma, P.le A. Moro 2, I-00185 Roma, Italy
[c] Dipartimento di Fisica, CNISM, CNIS, Sapienza Università di Roma, P.le A. Moro 5, I-00185 Roma, Italy
[d] Dip. Farmacia, Università "G.D'Annunzio", Via dei Vestini 31, 66100 Chieti, Italy
[e] Elettrochimica ed Energia, Via di Priscilla 22, I-00199 Roma, Italy

HIGHLIGHTS

- Iron oxide nanowires are characterizated as anode material for lithium-ion battery.
- The anode has specific capacity of 800 mAh g^{-1} evolving at 0.9 V vs. Li.
- Morphological and structural variation during lithium-conversion process is studied.
- The material has low cost and environment compatibility.

ARTICLE INFO

Article history:
Received 16 November 2013
Received in revised form
20 December 2013
Accepted 1 January 2014
Available online 21 January 2014

Keywords:
Iron-oxide
Nanowires
Anode
Lithium-ion-battery

ABSTRACT

Iron oxide nanowires are synthesized and characterized as negative electrode for lithium ion battery. The lithium-conversion reaction of the material is studied by electrochemical techniques as well as by XRD and SEM. Lithium cells based on the electrode material evidence a reversible capacity of about 800 mAh g^{-1} and a multiple-step electrochemical process leading to the formation of amorphous compound. Furthermore, SEM analysis of the compound formed by direct lithium atoms deposition on the iron oxide nanowires clearly evidences the change of the electrode morphology upon formation of a lithiated phase. We believe that the data here reported may shed light on the properties of the iron oxide nanowires as high capacity anode for lithium ion battery.

1. Introduction

Recently, the development of alternative anode materials of enhanced capacity and safety level assumed key role in the development of high performance lithium ion batteries. Transition metal oxides, based on the conversion reaction with lithium, are among the most promising alternatives to the graphite conventionally used as anode in commercial lithium ion battery [1] that is nowadays considered the best candidate to fulfill the strict requirements of emerging applications such as hybrid and electric cars and energy plants [2].

The conversion mechanism involves the exchange of more than one electron for redox center, thus allowing a higher specific capacity and energy density in comparison with the conventional electrodes based on lithium ions intercalation/de-intercalation. Among the various transition metal oxides, Iron (III) oxide Fe_2O_3 has attracted great interest in this field of research not only due to its good electrochemical properties (i.e. theoretical specific capacity of 1007 mAh g^{-1}) but also due to its very low cost and eco-sustainability [3]. In lithium cell, Fe_2O_3 electrode reacts through a complex mechanism consisting in the progressive intercalation of lithium ions in the three-dimensional electrode structure and, subsequently, in the conversion of Fe_2O_3 to metal Fe and Li_2O.

Considering the cell discharge process, the Fe_2O_3 electrochemical reaction can be described, according to literature papers [4], by the following steps:

$$Fe_2O_3 \rightarrow LiFe_2O_3 \rightarrow Li_2Fe_2O_3 \rightarrow 2Fe + 3Li_2O$$

* Corresponding author.
E-mail address: jusef.hassoun@uniroma1.it (J. Hassoun).

0378-7753/$ – see front matter © 2014 Elsevier B.V. All rights reserved.
http://dx.doi.org/10.1016/j.jpowsour.2014.01.052

The overall electrochemical process implies the exchange of 6 electrons for redox center and, therefore, a value of specific capacity much higher than the one shown by conventional anodes (i.e. 1007 mAh g^{-1} for Fe_2O_3 and 370 mAh g^{-1} for graphite).

However, Fe_2O_3 and other conversion electrodes are still far from being implemented as anodes in lithium ion batteries due to several problems limiting their performances in practical cells [5]. Structural re-organization experienced by the electrode during conversion reaction leads to de-cohesion and segregation of the Fe and Li_2O phases and, in the worst cases, to the pulverization of the electrode. This issue implies unsatisfactory charge–discharge efficiency of the cell and low capacity retention over cycling. In order to overcome these limits and make the transition metal oxide a viable electrode for lithium ion battery application many efforts have been recently made, mainly within the material engineering research field. A promising solution to reduce the volume changes of the electrodes during the electrochemical process consisted is the addition of a buffer matrix to the active material. It has also been demonstrated that the oxide particle size and morphology strongly influence the electrode behavior in practical cells [6] and, therefore, many attempts have been addressed to the synthesis of size controlled transition metal oxide particles of different shapes [7,8]. Here we report the electrochemical study of a Fe_2O_3 – nanowires electrode with the aim of testing its applicability in lithium ion batteries and of shedding light on its reaction mechanism by using both electrochemical techniques, such as galvanostatic cycling, potentiodynamic cycling and voltammetry, and chemical–physical techniques such as XRD and SEM.

2. Experimental

Hard template, mesoporous silica (SBA-15) was synthesized by the sol–gel method using a nonionic surfactant (EO20PO70EO20). SBA-15 was synthesized by the sol–gel method using a nonionic surfactant, $EO_{20}PO_{70}EO_{20}$ (EO and PO denote the ethyleneoxide and propyleneoxide unit, average Mw = 5800, Aldrich). Tetraethyl orthosilicate was added to the surfactant aqueous solution in which the pH was adjusted to 1.0 using 36% HCl. The mixture was then stirred at 35 °C for 24 h, and kept in a convection oven at 80 °C for 24 h. The reactant was filtrated, and the precipitate was annealed at 600 °C in a muffle. For embedding Fe_2O_3 in mesoporous silica, $Fe(NO_3)_3 \cdot 9H_2O$ 0.01 M was dissolved in 50 ml of ethanol and added to 1 g of SBA-15. The slurry was stirred at room temperature and then dried at 40 °C for 1 week. The so obtained brown colored powder was sintered at 550 °C for promoting NO_x decomposition and dehydration. The powder was following etched by 2 M NaOH solution for 6 h, washed and filtered several times. Finally, pure nanwires-agglomeration of Fe_2O_3 (following called with the acronym NWF) was obtained after drying at 60 °C.

The NWF anodes were prepared as thin films by casting on copper support a slurry composed by the active material (80% wt), PVdF 6020 Solvay binder (10% wt) and MMM Belgium Super-P carbon electronic conducting additive (10% wt).

XRD measurements were performed using a Rigaku D-max X-ray diffractometer equipped with a Cu-Kα radiation source. The Rietveld refinement of the XRD electrochemical data was performed by using the data analysis program MAUD. The fitting of the experimental pattern has been performed by considering the hematite (JCPDS # 86-2368) and maghemite (JCPDS # 24-0081) Fe_2O_3 phases. The fitting procedure was characterized by an acceptable RW agreement factor (<20%). The phase ratio has been determined as a result of this Rietveld analysis.

Swagelok t-type lithium half cells were assembled using a lithium metal foil counter electrode and a Whatman™ separator soaked with 1 M $LiPF_6$ Ethylene Carbonate–Dimethyl Carbonate (EC:DMC = 1:1 Merk Battery Grade) electrolyte solution.

The galvanostatic cycling tests were performed in the voltage range 0.3 V–3 V vs Li^+/Li using a Maccor 4000 series Battery Test System.

Cyclic Voltammetry (CV) tests were performed using lithium half cells with a lithium metal reference electrode at a scan rate of 0.1 mV s^{-1} within the 0.3–3 V vs. Li^+/Li potential range using a Bistat Biologic-Science Instruments potentiostat–galvanostat. All

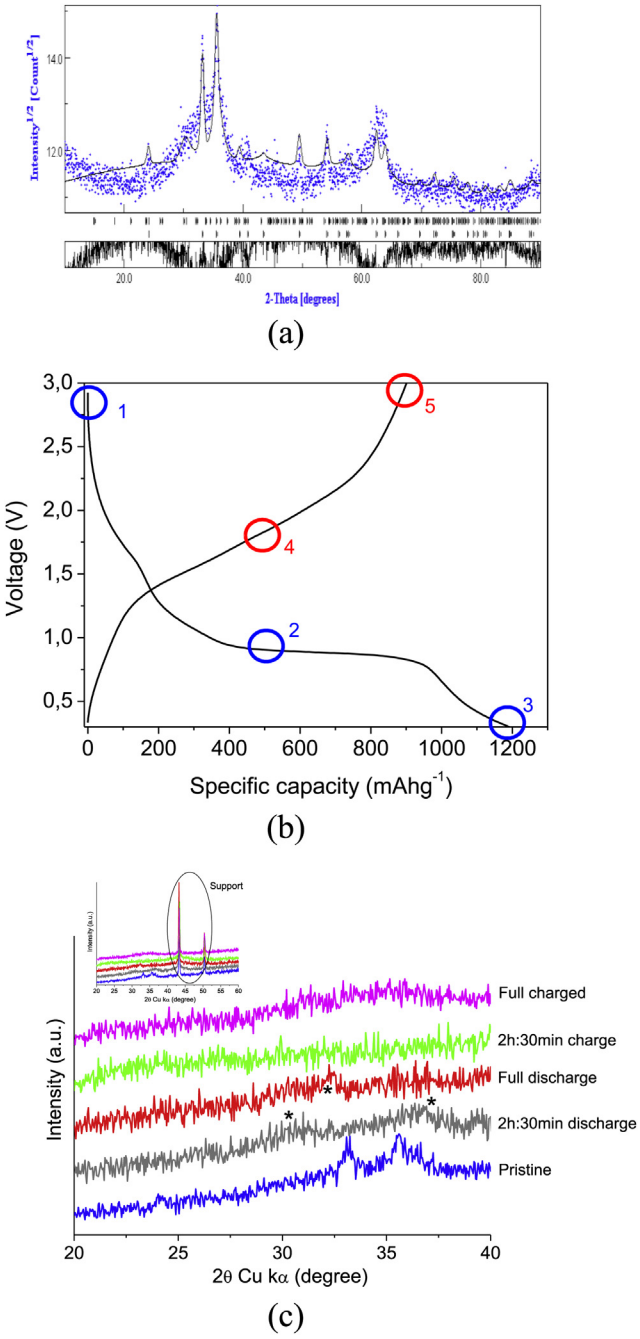

Fig. 1. (a) NWF powder experimental XRD pattern (blue) and computed spectra (black) obtained by the Rietveld refinement of diffraction data. (b) Voltage vs. specific capacity profile of the Li/EC:DMC, $LiPF_6$ 1M/NWF cell and (c) ex-situ XRD patterns of the corresponding NWF electrode upon cycling, within inset the signals of the electrode current collector. Voltage range 0.3–3 V, C/5 rate ($C_{theoretical}$ = 1007 mAh g^{-1}). (For interpretation of the references to colour in this figure legend, the reader is referred to the web version of this article.)

the cells tested were assembled under inert conditions in Argon-filled glove-box and all the electrochemical tests were performed at room temperature.

The SEM images of the nanowires were taken with a Zeiss Auriga 405 instrument at a beam energy of 10 KeV and at a working distance of 3.3 mm, with 1.0 nm nominal resolution at maximum magnification (600,000 X). The as-prepared iron-oxide nanowires were deposited on a Cu substrate from an ethanol solution with a Pasteur pipette. Samples were promptly insert into UHV and after a mild annealing at 80 °C, were exposed to lithium, by means of SAES Getters dispensers. SEM images were collected to compare the nanowires evolution after the lithiation procedure.

3. Results and discussion

The Rietveld refinement of the XRD pattern obtained using the NWF powder, reported in Fig. 1a, suggests the co-presence in the sample of two Fe_2O_3 phases, i.e. the hematite and maghemite, respectively, with a 50.6:49.4 weight ratio. Furthermore, the refinement indicates a Fe_2O_3 crystallite dimension of 70 ± 30 nm. However, heterogeneous distribution of the phases promoting higher ratio of one of the two phases, i.e. γ-Fe_2O_3 phases maghemite, cannot be excluded (XPS data not reported here).

Fig. 1b and c show the first galvanostatic lithiation/de-lithiation process in a lithium cell of the electrode prepared using the iron oxide nanowires powder as the active material in terms of voltage profile and the corresponding evolution of the electrode structure as evaluated by ex-situ XRD technique, respectively. The typical voltage signature of the iron oxide conversion reaction [9] can be observed in Fig. 1b, with lithiation process mainly evolving at about 0.9 V vs. Li and characterized by a capacity of the order of 1200 mAh g^{-1}, that is exceeding the theoretical value of the process in view of the SEI film formation process with corresponding electrolyte decomposition [10]. During the following de-lithiation process the cell voltage shows a sloppy signature centered at about 1.7 V vs. Li, with a reversible capacity as high as 930 mAh g^{-1}, i.e. 93% of the theoretical value. The patterns of the pristine electrode (reported in blue in Fig. 1c) show only some of the characteristic peaks of the Fe_2O_3, such as those at about 33 and 36° with limited resolution, this mainly due to the electrode nature and to the presence of strong signals related with the copper current collector (see inset of Fig. 1c). The above mentioned peaks gradually vanish upon lithiation to finally disappear at the end of the process (gray and green patterns in Fig. 1c). Furthermore, the appearance of additional peaks, indicated with asterisks in Fig. 1c, most likely indicates the formation of Li–Fe–O intermediate compounds. However the very low intensity of these peaks avoids the determination of the Li:Fe:O atomic ratio. The following de-lithiation process shows the complete disappearance of the peaks, with formation of an amorphous compound. These results, evidencing a progressive amorphization of the Fe_2O_3 phase over the lithiation–delithiation process, make difficult the identification of the compounds formed during the process by ex-situ XRD technique using the electrochemically cycled electrodes. Meanwhile, in our previous paper [9] we reported that XRD patterns of the lithiated crystalline Fe_2O_3 evidences amorphous phase with only some residual peaks related to traces of α-Fe_2O_3 and it appeared very difficult to speculate on the presence of Li_2O, i.e. the other assumed product of the electrochemical reaction. To be remarked that the ex-situ XRD patterns here reported show a relatively low signal/noise ratio, mainly due to the nature of the

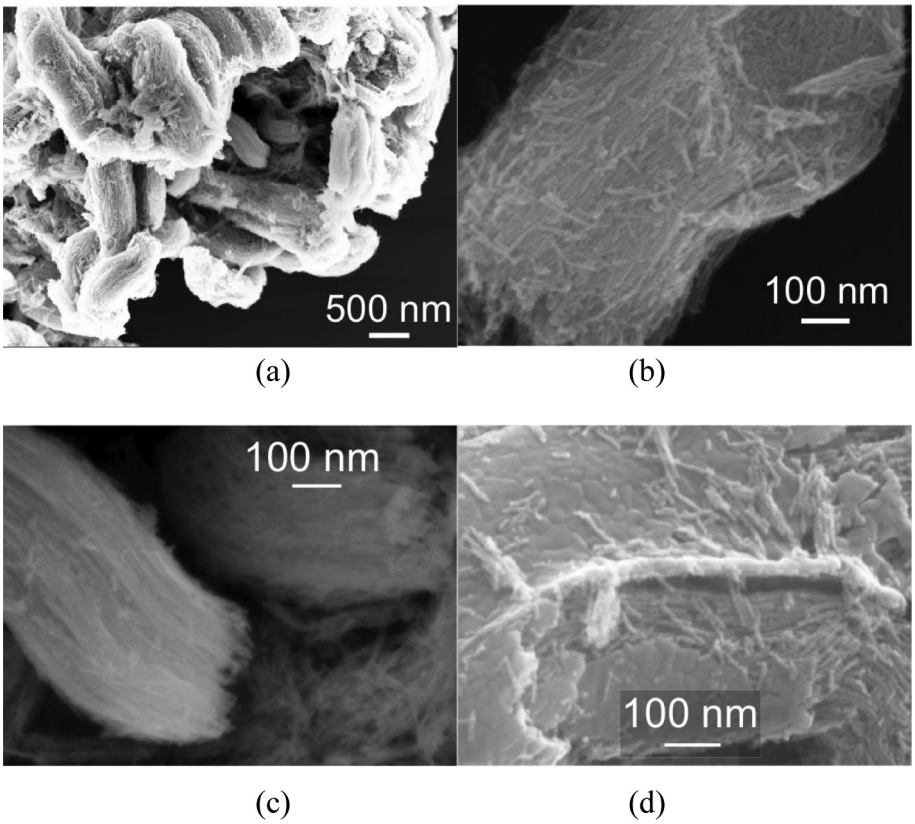

Fig. 2. SEM images NWF powder in the pristine state (a) and its magnification (b). SEM images of the NWF before (c) and after (d) physical lithiation, reported with the same magnification.

electrode. However, by using these patterns we can qualitatively evaluate the disappearance of the main Fe_2O_3 phase peaks upon cycling, without speculating on electrode reaction mechanism that certainly requires additional study.

A further investigation of the lithiation process has then been performed by mean of SEM analysis of NWF powder physically lithiated. The effect of the lithiation process over the NWF powder morphology is shown in the SEM images of Fig. 2. The image evidences that the sample is formed by sheet-like micrometric agglomeration (Fig. 2a) of nanowires (magnification in Fig. 2b) and that the original particle size (Fig. 2c) is remarkably increased by physical lithiation process, with partial coalescence of the wires in the particle surface and bulk (Fig. 2d) such as by the effect of "lithium-insertion" into NWF structure, as already expected by the lithium-conversion electrochemical process [5] and demonstrated by XPS (data not reported here).

A more detailed electrochemical study of the NWF electrochemical process has been performed by cyclic voltammetry. Fig. 3a, reporting the voltammogram of the three electrode lithium cell assembled using the NWF electrode, shows three peaks centered at about 1.65 V, 1.1 V and 0.85 V vs. Li^+/Li during the first lithiation process. Previous works demonstrated that the peaks at about 1.65 V and 1.1 V may be associated with the intercalation of the lithium ions in the Fe_2O_3 electrode structure and formation of $LiFe_2O_3$ and $Li_2Fe_2O_3$ phases, respectively, while the peak located at about 0.85 V

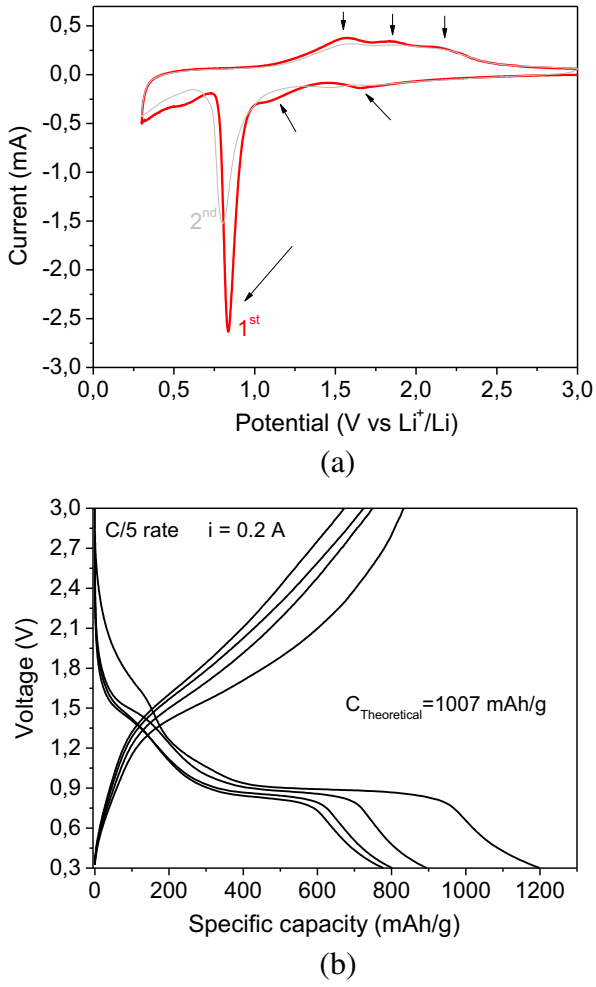

Fig. 3. (a) Cyclic voltammetry of the NWF electrode in a Li/EC:DMC, $LiPF_6$ 1M/NWF cell. Potential range: 0.3–3 V. (b) Voltage profile of a Li/EC:DMC, $LiPF_6$ 1M/NWF cell cycled in the 0.3–3 V voltage range at C/5 rate ($C_{theoretical}$ = 1007 mAh g^{-1}).

is attributed to the conversion reaction of Fe_2O_3 to metallic Fe and Li_2O[9]. Moreover, the CV profile of Fig. 3a shows an additional peak at about 0.6 V, most likely associated with the electrolyte decomposition with corresponding SEI film formation [10]. During the following anodic scan, the electrochemical de-lithiation process shows peaks centered at 1.6 V, 1.85 and 2.2 V vs Li^+/Li, respectively, thus confirming the mixed intercalation-conversion mechanism characteristic of the Li–Fe_2O_3 reaction. The above described peaks, except that associated with SEI formation, can be observed during the subsequent lithiation-delithiation cycles (reported in gray color in Fig. 3a), however with broader, less defined shape and slightly shifted potential values.

The practical use of the NWF is preliminary demonstrated by galvanostatic cycling tests in a Li/EC:DMC, $LiPF_6$ 1M/NWF cell at room temperature, see Fig. 3b. The voltage signature shows a charge/discharge profile that is in good agreement with the CV curves previously discussed, with lithium intercalation process evolving at about 1.7 V and conversion at about 0.85 V during the discharge, and sloppy profile with merged plateaus and average voltage of about 1.7 V during the charge. Furthermore, Fig. 3b indicates a reversible capacity of about 800 mAh g^{-1} during the following cycles, with excess capacity during the first cycle associated with the already discussed SEI film formation, and resulting charge–discharge efficiency of 70% during the first cycle increasing to about 85–90% in the subsequent cycles. However, the cell shows certain capacity decay during cycling as most likely attributed to a still not optimized electrode structure and consequent segregation of the Fe and Li_2O phases during the NWF conversion reaction. Certainly, further efforts are required in order to enhance the NWF electrochemical behavior, such as the addition to the active material of carbon-based buffers able to limit the volume changes characteristic of the electrode conversion reaction.

4. Conclusion

The results obtained in this study shed light on the NWF anode electrochemical behavior in a lithium cell and evidence that its reaction mechanism is based on both lithium ions intercalation and conversion chemistry. All the tests performed confirm the applicability of this material as anode in lithium ion batteries. Many issues have still to be addressed in order to make the NWF suitable electrode, however the results here reported suggest its potential applicability as high capacity, low cost and environmentally compatible anode in lithium ion battery.

Acknowledgment

This work was supported by the Italian Institute of Technology (Project "REALIST" Rechargeable, advanced, nano structured lithium batteries with high energy storage) and by the "Regione Lazio", Italy. We thank Francesco Mura at the SNN-Lab for performing SEM images.

References

[1] P. Poizot, S. Laurelle, S. Grugeon, L. Dupont, J.M. Tarascon, Nature 407 (2000) 496.
[2] B. Scrosati, J. Hassoun, Y.K. Sun, Energy Environ. Sci. 4 (2011) 3287.
[3] Y. Ding, J. Li, Y. Zhao, L. Guan, Mater. Lett. 81 (2012) 105.
[4] D. Larcher, D. Bonnin, R. Cortes, I. Rivals, L. Personnaz, J.-M. Tarascon, J. Electrochem. Soc. 150 (2003) A1643.
[5] J. Cabana, L. Monconduit, D. Larcher, M.R. Palacin, Adv. Energy Mater. 22 (2010) E170.
[6] K.M. Shaju, F. Jiao, A. Débart, P.G. Bruce, Phys. Chem. Chem. Phys. 9 (2007) 1837.
[7] Z.Y. Wang, D.Y. Luan, S. Madhavi, C.M. Li, X.W. Lou, Chem. Commun. 47 (2011) 8061.
[8] Y.M. Lin, P.R. Abel, A. Heller, C.B. Mullins, J. Phys. Chem. Lett. 2 (2011) 2885.
[9] J. Hassoun, F. Croce, I. Hong, B. Scrosati, Electrochem. Commun. 13 (2011) 228.
[10] D. Aurbach, J. Power Sources 89 (2000) 206.